

Pathways to Immonium Ions in the Fragmentation of Protonated Peptides

Kishani Ambihapathy, Talat Yalcin, Hei-Wun Leung† and Alex G. Harrison*

Department of Chemistry, University of Toronto, Toronto, Ontario, M5S 3H6, Canada

The pathways leading to the formation of immonium (A_n) ions in the fragmentation of protonated peptides were investigated using metastable ion studies, including kinetic energy release measurements, and low-energy collision-induced dissociation studies. In addition to the established pathway $B_n \rightarrow A_n + CO$, it is shown that B_2 ions, in suitable circumstances, fragment directly to A_1 ions. In addition, metastable ion studies show that A_1 ions can be formed directly from protonated di- and tripeptides most likely by concerted elimination of CO and an amino acid or smaller peptide. A_2 ions can be formed directly from protonated dipeptides in part through the sequential loss of $H_2O + CO$, although kinetic energy release measurements suggest direct elimination of HCOOH also may be occurring. Internal immonium ions are shown to originate by further fragmentation of A_n ions and by further fragmentation of Y_n'' ions. © 1997 by John Wiley & Sons, Ltd.

J. Mass Spectrom. 32, 209–215 (1997)

No. of Figures: 14 No. of Tables: 5 No. of Refs: 37

KEYWORDS: immonium ions; metastable ions; kinetic energy release; protonated peptides

INTRODUCTION

Tandem mass spectrometry^{1,2} plays an increasingly important role in determining the amino acid sequence of peptides. As a result, the main types of ions observed in the fragmentation of protonated peptides are well established,^{3–8} as illustrated schematically in Fig. 1, although relatively few detailed mechanistic studies have been carried out. The present study is concerned with the mechanisms by which immonium ions are formed in the fragmentation of protonated peptides. It

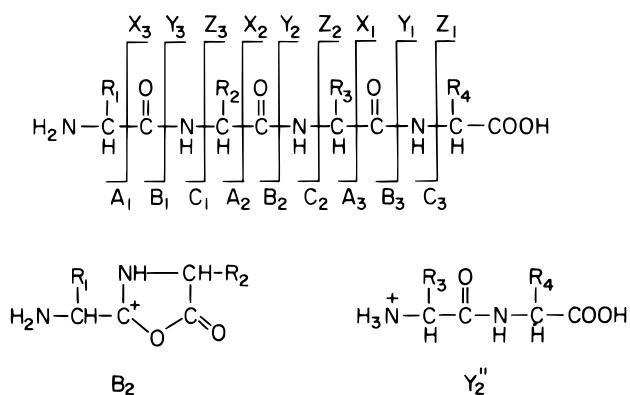


Figure 1. Schematic diagram of major fragmentation reactions of protonated peptides.

* Correspondence to: A. G. Harrison.

† Visiting Professor 1995. Permanent address: Department of Chemistry, Hong Kong Baptist University, Kowloon, Hong Kong.
Contract grant sponsor: Natural Sciences and Engineering Research Council (Canada).

has been generally assumed^{9–11} that A_n ions are formed by elimination of CO from the corresponding B_n ions and, indeed, this is one pathway to immonium ion formation.^{12,13} However, as noted recently by Speir and Amster,¹⁴ there are occasions when immonium ions are observed in the absence of the corresponding B ion. In addition, immonium ions ($RCH=NH_2^+$) characteristic of the amino acids present in the peptide frequently are observed at low masses in the collision-induced dissociation (CID) mass spectra of protonated peptides,^{9,15–19} which cannot arise simply by loss of CO from B ions formed in the primary amide bond cleavage reaction. In the present study we have used metastable ion studies^{20,21} and energy-resolved collisional mass spectrometry^{22–24} to probe the pathways by which A_n ions, particularly A_1 ions, are formed in the fragmentation of small protonated peptides. These studies provide information as to possible pathways to A_n ions and also to internal immonium ions in the spectra of larger peptides. This will be illustrated with reference to the formation of immonium ions in the fragmentation of protonated leucine enkephalin (H-Tyr-Gly-Gly-Phe-Leu-OH).

EXPERIMENTAL

All experimental work was carried out using a ZAB-2FQ hybrid BEqQ mass spectrometer (VG Analytical, Wythenshawe, Manchester, UK) which has been described in detail previously.²⁵ Briefly, this instrument is a reversed-geometry (BE) double-focussing mass spectrometer that is followed by a deceleration lens system, an r.f.-only quadrupole collision cell (q) and a quadrupole mass analyzer (Q). The ions studied were

prepared by fast atom bombardment (FAB) using an argon atom beam of 7–8 keV energy with the appropriate sample dissolved in a matrix consisting of thioglycerol–2,2'-dithiodiethanol (1:1) saturated with oxalic acid.

To obtain the relative abundances of fragment ions formed on the metastable ion time-scale, the precursor ion of interest was mass selected by the BE double-focusing mass spectrometer at 6 keV ion energy, decelerated to 20–40 eV kinetic energy and introduced into the r.f.-only quadrupole cell in the absence of collision gas. Low-energy collision-induced dissociation (CID) studies were carried out in the same fashion but with the addition of N₂ at an indicated pressure of $\sim 2 \times 10^{-7}$ Torr (1 Torr = 133.3 Pa) to the quadrupole collision cell. In the CID experiments the incident ion energy typically was varied from 2 to 45 eV (laboratory scale). In both the unimolecular and CID studies the ionic fragments were analyzed by scanning the final quadrupole Q with, typically, 20–30 2 s scans being accumulated on a multi-channel analyzer. The energy-resolved CID data are presented in the following in the form of breakdown graphs expressing the relative fragment ion signals as a function of the collision energy.

In several cases the precursors to immonium ions were examined by reaction intermediate scans.²⁶ In this approach the MH⁺ ion was mass selected by the magnetic sector, the quadrupole mass analyzer (Q) was set to transmit the immonium ion of interest and the electric sector was scanned to record the intermediate ions leading to formation of the immonium ion.

Kinetic energy releases associated with the unimolecular fragmentation reactions were determined by the mass analyzed ion kinetic energy spectrometric (MIKES) technique.²⁰ In this technique the ion of interest was mass selected by the magnetic sector at 6 keV ion energy and the ionic products of unimolecular fragmentation reactions in the drift region between the magnetic and electric sectors were identified according to their kinetic energy by scanning the electric sector. The kinetic energy releases were determined from the peak widths at half-height, after correction for the inherent energy spread of the ion beam according to the relation²¹

$$w_{\text{corr}} = (w_{\text{met}}^2 - w_{\text{mb}}^2)^{1/2} \quad (1)$$

where w_{met} is the measured width of the metastable peak and w_{mb} is the width of the parent ion beam. The corrected half-widths were converted into $T_{1/2}$ values using the equation developed²⁰ for electric sector scans.

The compounds used were obtained from Aldrich Chemical, Sigma Chemical and Bachem Biosciences and were used as received.

RESULTS AND DISCUSSION

A_n sequence ions and internal immonium ions (I) are observed most frequently for peptides containing aromatic and aliphatic amino acids; accordingly, we limited this study primarily to small peptides containing the Phe, Tyr, Pro, Val and Leu residues. We discuss in

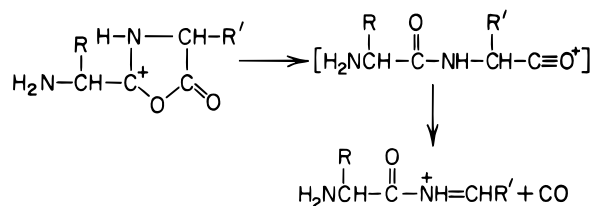
detail below the various pathways to these A_n and internal immonium ions.



The formation of immonium ions by the fragmentation reaction



has been studied in detail in earlier work.^{12,13} We have shown that the stable B_n ions have a protonated oxazolone structure and that fragmentation occurs as outlined in Scheme 1 with the acyclic acylium ion as a transient intermediate. Loss of CO from the transient acylium ion is exothermic with the result that the fragmentation reaction occurs on the metastable ion time-scale with substantial release of kinetic energy ($T_{1/2} = 0.3\text{--}0.5$ eV). This fragmentation pathway is illustrated in Fig. 2 which shows the breakdown graph for protonated H-Gly-Tyr-Gly-OH. Initial fragmentation of the protonated peptide occurs exclusively by elimination of neutral glycine to give the B₂ ion which, at higher collision energies, eliminates CO to give the A₂ ion at m/z 193. As shown in Table 1, metastable ion fragmentation of the protonated peptide gave exclusively the B₂ ion.



Scheme 1.

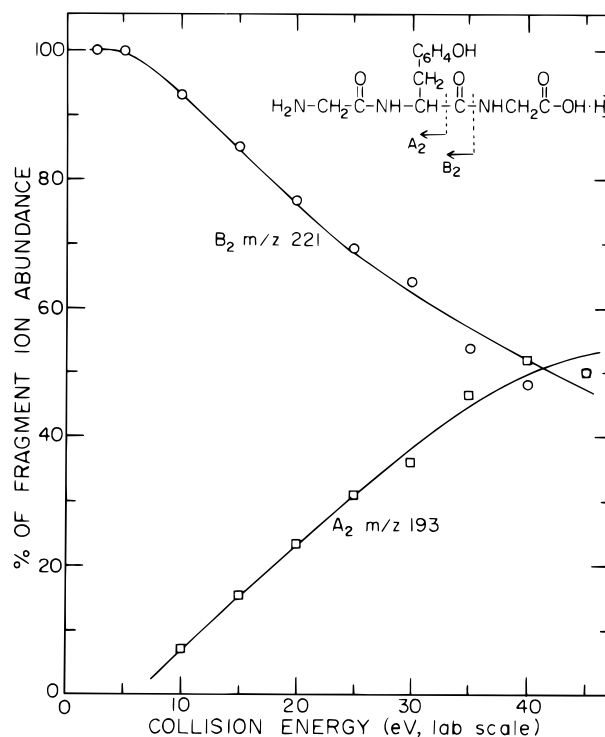


Figure 2. Breakdown graph for protonated H-Gly-Tyr-Gly-OH.

derived from H-Leu-Gly-Gly-OH and from H-Leu-Gly-NH₂, reported in Ref. 12, but was not commented upon at that time. Clearly, formation of the A₁ ion is in competition with formation of the A₂ ion and the relative importance of the two fragmentation reactions of the B₂ ion will depend on the relative stabilities of the A ions formed. The fragmentation channel illustrated by Scheme 2 may also exist for larger B_n ions, although we have not observed it experimentally. For larger B_n ions, an alternative fragmentation is to form the next lower B ion, B_{n-1}. Thus, the B₃ ion derived from H-Tyr-Gly-Gly-Phe-Leu-OH fragments primarily to the B₂ ion while the B₄ ion derived from the same peptide fragments to form both the A₄ and the B₃ ion.¹³

The breakdown graph for the B₃ ion of leucine enkephalin¹³ shows that the B₂ ion formed fragments further to form the A₁ ion by the route outlined in Scheme 2 and this represents a major route to the N-terminal immonium ion in the fragmentation of protonated leucine enkephalin. This sequence, B₃ → B₂ → A₁, is also evident from the tandem mass spectral studies of Cheng *et al.*²⁸

MH⁺ → A₁ + neutral(s)

The data in Tables 1 and 2 show metastable ion signals for formation of the A₁ immonium ion by fragmentation of MH⁺ when the N-terminal amino acid of the peptide is Val, Phe, Pro, Tyr or Leu. These unimolecular fragmentation reactions have also been observed by Kulik and Heerma^{29,30} in MIKES²⁰ studies of the fragmentation of selected dipeptides and tripeptides. The relative metastable ion abundances they reported are given in parentheses in Tables 1 and 2 for peptides which were common to both studies. There are substantial differences in relative abundances presumably reflecting the different time intervals (and, hence,

Table 2. Metastable ion fragmentation of protonated dipeptides^a

Peptide	Fragment ion (% of base peak)			
	B ₂	A ₂	A ₁	Y ₁ ^{''}
H-Phe-Val-OH ^b	9 (56)	19 (20)	100 (100)	6
H-Val-Phe-OH	2 (72)		100 (42)	60 (100)
H-Phe-Gly-OH	2		100	
H-Gly-Phe-OH	61	93		100
H-Tyr-Gly-OH ^c			100	
H-Gly-Tyr-OH	44	100		95
H-Pro-Gly-OH			100	
H-Gly-Pro-OH	10	19		100
H-Phe-Tyr-OH	4	6	100	52
H-Tyr-Phe-OH	47	1	100	16
H-Phe-Leu-OH ^d	14 (68)	20 (18)	100 (100)	

^a Abundances in parentheses from Ref. 29, as measured by MIKES.

^b Ref. 29 reports [MH⁺ - NH₃]⁺ = 31.

^c [MH⁺ - NH₃]⁺ = 46.

^d Ref. 29 reports [MH⁺ - NH₃]⁺ = 43.

internal energy distributions of MH⁺) sampled by the MIKES technique on a ZAB BE mass spectrometer^{29,30} and by quadrupole scans on the ZAB-2FQ BEqQ mass spectrometer used in the present work. It might be noted that Kulik and Heerma²⁹ also reported substantial formation of A₁ ions by fragmentation of a variety of dipeptides in addition to those we have studied; these included H-Leu-Phe-OH, H-Pro-Leu-OH, H-Val-Tyr-OH, H-Tyr-Val-OH, H-Ala-Gly-OH and H-Pro-Val-OH. It is clear from the data in Tables 1 and 2 and from the data reported by Kulik and Heerma^{29,30} that the formation of A₁ ions by fragmentation of MH⁺ is more prevalent for dipeptides than for tripeptides. In the latter case, alternative fragmentation channels to form B₃, B₂ and Y₁^{''} ions are more common unless the A₁ immonium ion is particularly stable (i.e. derived from N-terminal tyrosine, phenylalanine or proline). Direct formation of the A₁ ion also is indicated by the breakdown graph of protonated H-Tyr-Gly-Gly-OH presented in Fig. 5.

The identity of the neutral(s) accompanying the formation of the A₁ ion in these cases is not entirely clear. Protonated amino acid derivatives, H₂NCH(R)C(=O)X·H⁺ (X = OH, NH₂, OCH₃), show dominant fragmentation to form immonium ions^{12,31-36} and, on the metastable ion time-scale, this fragmentation reaction is accompanied by a substantial release of kinetic energy (T_{1/2} = 0.3-0.5 eV).^{12,33,34} It generally has been proposed^{12,32} that the fragmentation reaction proceeds in a stepwise fashion as illustrated in Scheme 3. Thermochemical estimates^{32,35} indicate that the enthalpy of formation of the intermediate acylium ion, H₂NCH(R)CO⁺, is higher than that of the products RCH=NH₂⁺ + CO and, by analogy with the results for fragmentation of larger B ions, which show^{12,13} T_{1/2} = 0.4-0.5 eV for elimination of CO, it is

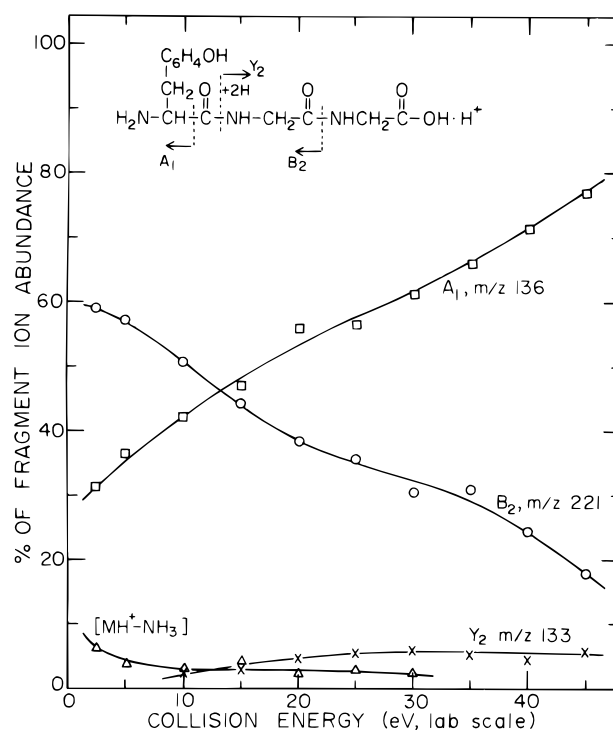
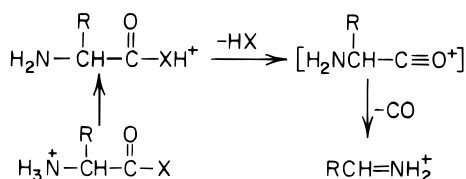
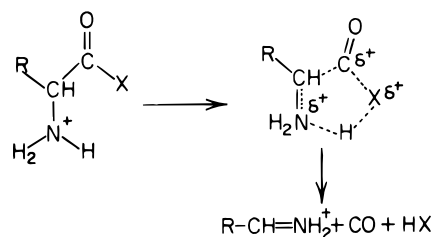


Figure 5. Breakdown graph for protonated H-Tyr-Gly-Gly-OH.



Scheme 3.

likely that the kinetic energy release originates in this step. Thus, if the A_1 ion in the spectra of the dipeptides and tripeptides originates by the pathway outlined in Scheme 3 (HX = amino acid or dipeptide), one might have expected kinetic energy releases in metastable ion fragmentation in the range 0.3–0.4 eV, similar to that observed for formation of immonium ions from protonated amino acid amides.¹² However, as shown by the results in Table 3, the kinetic energy release in formation of the A_1 ion from the protonated dipeptides and tripeptides is small and would appear to preclude the stepwise mechanism of Scheme 3. We believe that this mechanism is incorrect in detail. Table 4 records the $T_{1/2}$ values measured for metastable ion formation of the immonium ion $C_6H_5CH_2CH=NH_2^+$ from a variety of protonated phenylalanine derivatives, H-Phe-X. The most striking feature is that the kinetic energy release decreases from 0.36 eV when $X = OH$ to 0.15 eV when $X = OC_2H_5$ and decreases even further (Table 3) when $X = NHCH_2COOH$ or $NHCH_2CONHCH_2COOH$. These results are not consistent with a stepwise mechanism in which the kinetic energy release originates in the CO-elimination step. A possible rationalization of these results is that the reaction is concerted and that the departing HX is still interacting with and stabilizing the acylium ion as the C—CO bond is broken (Scheme 4). A similar mechanism has been suggested by Bouchoux *et al.*³⁵ Note that the kinetic energy release decreases as the size (and, hence, the polarizability) of the HX group increases. Thus, it seems most likely that the A_1 ions are formed directly from the protonated dipeptides and tripeptides by the con-



Scheme 4.

certed mechanism outlined in Scheme 4. An additional route to the A_1 ion could involve the intermediate formation of the B_2 ion which fragments further (Scheme 2) to form the A_1 ion when this immonium ion is particularly stable. However, in a number of cases (H-Tyr-Gly-OH, H-Pro-Gly-OH) metastable ion formation of A_1 is observed without any metastable ion formation of the B_2 ion. Further, for protonated H-Phe-Gly-Gly-OH and H-Tyr-Gly-Gly-OH, reaction intermediate scans showed no evidence for the sequential metastable ion fragmentation reaction $MH^+ \rightarrow B_2 \rightarrow A_1$.

As the final entry in Table 2 shows, the dominant metastable ion fragmentation reaction of protonated H-Phe-Leu-OH (the Y_2'' ion of leucine enkephalin) involves formation of the A_1 ion, $C_6H_5CH_2CH=NH_2^+$; this also is the major product in the CID spectrum. Since the Y_2'' ion is formed in the CID of protonated leucine enkephalin,^{13,27,28} this probably is a significant route to the interior immonium ion ($F - 28$, m/z 120) that also is observed.

Dipeptide $\cdot H^+ \rightarrow A_2 + \text{neutral(s)}$

The data in Table 2 show that in a number of cases, particularly H-Phe-Val-OH, H-Gly-Phe-OH, H-Gly-Tyr-OH and H-Gly-Pro-OH, there is a metastable ion signal for formation of the A_2 ion by fragmentation of the MH^+ ion. A similar conclusion is reached by examination of the breakdown graph for protonated H-Gly-Phe-OH shown in Fig. 6. A precursor ion scan for the m/z 177 (A_2) ion from protonated H-Gly-Phe-OH showed (Fig. 7) both m/z 223 (MH^+) and m/z 205 (B_2) as precursors in metastable ion formation of the A_2 ion. Thus, at least part of the A_2 metastable ion signal originates by the pathway shown in Scheme 3 ($HX = H_2O$) involving intermediate formation of the B_2 ion. However, kinetic energy release measurements indicate that this is not the only pathway operative. The relevant data for the H-Gly-Phe-OH and H-Gly-Tyr-OH systems are presented in Table 5, from which it can be seen that the measured kinetic releases for the reaction $MH^+ \rightarrow A_2$ are considerably smaller than those for the step $B_2 \rightarrow A_2 + CO$, in contrast to what is predicted for sequential metastable ion fragmentation reactions.³⁷ This implies that there is a second route to A_2 involving

Table 3. Kinetic energy releases ($T_{1/2}$) in formation of A_1 ions from MH^+ of dipeptides and tripeptides

Peptide	m/z (A_1)	$T_{1/2}$ (eV)
H-Tyr-Gly-OH	136	0.067
H-Tyr-Gly-Gly-OH	136	0.044
H-Phe-Val-OH	120	0.046
H-Phe-Gly-OH	120	0.078
H-Phe-Gly-Gly-OH	120	0.041
H-Pro-Gly-Gly-OH	70	0.050

Table 4. Kinetic energy releases in formation of immonium (A_1) ion from protonated phenylalanine derivatives

H-Phe-X	$T_{1/2}$ (eV)
H-Phe-OH	0.36
H-Phe-NH ₂	0.30
H-Phe-OCH ₃	0.22
H-Phe-OC ₂ H ₅	0.15

Table 5. $T_{1/2}$ values for fragmentation of protonated dipeptides

Peptide	$T_{1/2}$ (eV)		
	$MH^+ \rightarrow B_2$	$B_2 \rightarrow A_2$	$MH^+ \rightarrow A_2$
H-Gly-Phe-OH	0.030	0.34	0.18
H-Gly-Tyr-OH	0.039	0.33	0.21

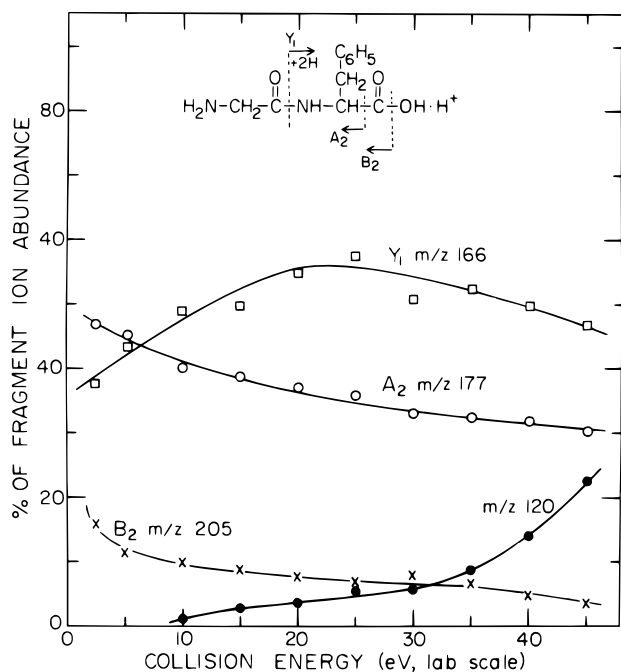
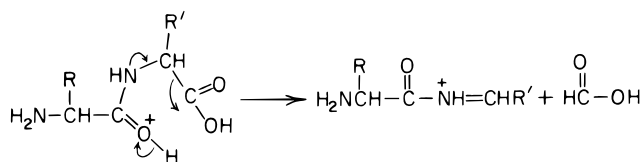


Figure 6. Breakdown graph for protonated H-Gly-Phe-OH.

a smaller kinetic energy release; a pathway involving direct elimination of HCOOH from MH^+ is suggested in Scheme 5.

Formation of internal immonium ions (I)

The breakdown graph of Fig. 3 for the B_2 ion derived from H-Gly-Phe-Gly-OH shows exclusive formation of the A_2 ion at low collision energies. However, as the collision energy increases there is substantial formation of m/z 120, the immonium ion derived from phenylalanine. Similar results were obtained for the B_2 ion derived from H-Gly-Tyr-Gly-OH, i.e. m/z 136, $HOC_6H_4CH_2CH=NH_2^+$, was observed at higher collision energies. A possible mechanism leading to this internal immonium ion is presented in Scheme 6.



Scheme 5.

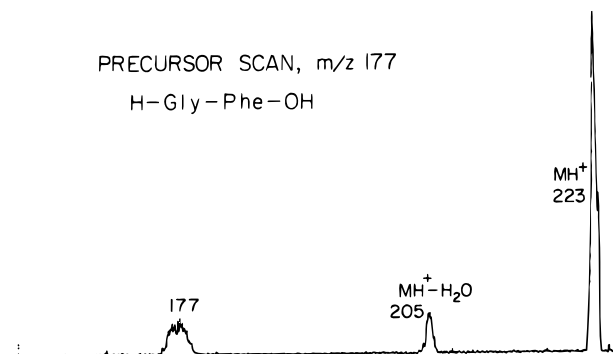
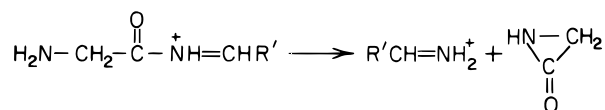


Figure 7. Precursor ion scan for m/z 177 (A_2) ion from protonated H-Gly-Phe-OH.



Scheme 6.

The breakdown graph in Fig. 6 illustrates another pathway to internal immonium ions. Protonated H-Gly-Phe-OH fragments to a considerable extent to form the Y_1 ion, protonated phenylalanine, which, at higher internal energies, fragments further by elimination of $H_2O + CO$, a reaction common to protonated amino acids,^{12,31-36} to form the internal immonium ion $C_6H_5CH=NH_2^+$ (m/z 120). Similar results were obtained for protonated H-Gly-Tyr-OH and protonated H-Gly-Pro-OH. As Fig. 8 shows, this reaction sequence also is important for tripeptides. Protonated H-Gly-Gly-Tyr-OH forms protonated tyrosine in high yield and this species fragments further at higher collision energies by loss of $H_2O + CO$ to give the internal immonium ion at m/z 136.

CONCLUSIONS

A number of pathways leading to immonium ions (A_n), in addition to the established pathway of loss of CO from B_n ions, have been elucidated. Of these, the most important is the formation of A_1 ions by fragmentation of B_2 ions. This appears to be a particularly important route for fragmentation of B_2 ions when the A_1 immon-

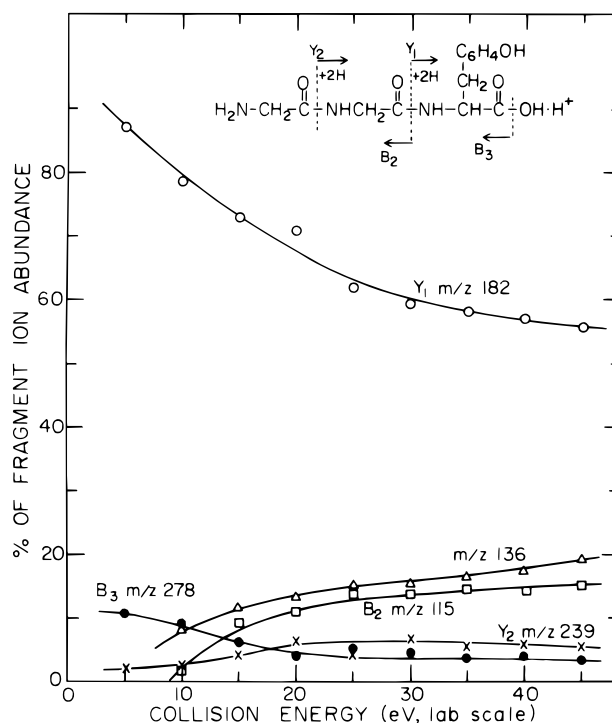


Figure 8. Breakdown graph for protonated H-Gly-Gly-Tyr-OH.

ium ion is stable and the A_2 ion formed by loss of CO has no particular claim to stability. Metastable ion studies also indicate formation of A_1 and A_2 immonium ions directly by fragmentation of protonated peptides. In the first case it is proposed that the fragmentation occurs directly from the MH^+ ion involving concerted elimination of CO plus an amino acid or smaller peptide. In the latter case it is suggested that, in addition to loss of $H_2O + CO$, direct elimination of formic acid probably occurs. Internal immonium ions are shown to be formed by fragmentation of Y_n'' ions, as might be expected from the known fragmentation of

protonated amino acids and from the fragmentation reactions of protonated peptides observed in the present work. It also is shown that internal immonium ions can be formed from A_n ions at higher internal energies.

Acknowledgements

The authors are indebted to the Natural Sciences and Engineering Research Council (Canada) for financial support and to VG Analytical for the loan of the FAB source and fast atom gun. H.-W. L. is grateful to the Hong Kong Baptist University for providing a sabbatical leave.

REFERENCES

1. F. W. McLafferty (Ed.), *Tandem Mass Spectrometry*. Wiley, New York (1983).
2. K. L. Busch, G. L. Glish and S. A. McLuckey, *Mass Spectrometry/Mass Spectrometry: Techniques and Applications of Tandem Mass Spectrometry*. VCH, New York (1988).
3. P. Roepstorff and J. Fohlman, *Biomed. Mass Spectrom.* **11**, 601 (1984).
4. D. F. Hunt, J. R. Yates, III, J. Shabanowitz, S. Winston and C. R. Hauer, *Proc. Natl. Acad. Sci. USA* **83**, 6233 (1986).
5. K. Biemann and S. Martin, *Mass Spectrom. Rev.* **6**, 75 (1987).
6. K. Biemann, *Biomed. Environ. Mass Spectrom.* **16**, 99 (1988).
7. K. Biemann, *Methods Enzymol.* **193**, 25 (1990).
8. K. Biemann, in *Biological Mass Spectrometry. Present and Future*, edited by T. Matsuo, R. M. Caprioli, M. L. Gross and Y. Seyama, p. 275, Wiley, New York (1993).
9. R. S. Johnson, S. A. Martin and K. Biemann, *Int. J. Mass Spectrom. Ion Processes* **86**, 137 (1988).
10. D. F. Hunt, J. Shabanowitz, J. R. Yates, III, R. R. Griffen and N.Z. Zhu, in *Mass Spectrometry of Biological Materials*, edited by C. N. McEwen and B. S. Larsen, Chapt. 5. Marcel Dekker, New York (1990).
11. A. E. Ashcroft and P. J. Derrick, in *Mass Spectrometry of Peptides*, edited by D. M. Desiderio, Chapt. 8. CRC Press, Boca Raton, FL (1991).
12. T. Yalcin, C. Khouw, I. G. Csizmadia, M. R. Peterson and A. G. Harrison, *J. Am. Soc. Mass Spectrom.* **6**, 1165 (1995).
13. T. Yalcin, I. G. Csizmadia, M. R. Peterson and A. G. Harrison, *J. Am. Soc. Mass Spectrom.* **7**, 233 (1996).
14. J. Speir and I. J. Amster, *J. Am. Soc. Mass Spectrom.* **6**, 1069 (1995).
15. W. Kausler, K. Schneider and G. Spiteller, *Biomed. Environ. Mass Spectrom.* **13**, 405 (1986).
16. R. S. Johnson and K. Biemann, *Biomed. Environ. Mass Spectrom.* **18**, 945 (1989).
17. T. Madden, K. J. Welham and M. A. Baldwin, *Org. Mass Spectrom.* **26**, 443 (1991).
18. A. M. Falick, W. M. Hines, K. F. Medzihradzky, M. A. Baldwin and B. W. Gibson, *J. Am. Soc. Mass Spectrom.* **4**, 882 (1993).
19. A. Papayannopoulos, *Mass Spectrom. Rev.* **14**, 49 (1995).
20. R. G. Cooks, J. H. Beynon, R. M. Caprioli and G. R. Lester, *Metastable Ions*. Elsevier, New York (1973).
21. J. L. Holmes and J. K. Terlouw, *Org. Mass Spectrom.* **15**, 383 (1980).
22. S. A. McLuckey, G. L. Glish and R. G. Cooks, *Int. J. Mass Spectrom. Ion Phys.* **39**, 219 (1981).
23. D. D. Fetterolf and R. A. Yost, *Int. J. Mass Spectrom. Ion Phys.* **44**, 37 (1982).
24. S. A. McLuckey and R. G. Cooks, in *Tandem Mass Spectrometry*, edited by F. W. McLafferty, p. 203, Wiley, New York (1983).
25. A. G. Harrison, R. S. Mercer, E. J. Reiner, A. B. Young, R. K. Boyd, R. E. March and C. J. Porter, *Int. J. Mass Spectrom. Ion Processes* **74**, 13 (1986).
26. J. N. Louris, L. G. Wright, R. G. Cooks and A. E. Schoen, *Anal. Chem.* **57**, 2918 (1985).
27. A. J. Alexander and R. K. Boyd, *Int. J. Mass Spectrom. Ion Processes* **90**, 211 (1989).
28. X. Cheng, Z. Wu, C. Fenselau, M. Ishihara and B. D. Musselman, *J. Am. Soc. Mass Spectrom.* **6**, 175 (1995).
29. W. Kulik and W. Heerma, *Biomed. Environ. Mass Spectrom.* **17**, 173 (1988).
30. W. Kulik and W. Heerma, *Biomed. Environ. Mass Spectrom.* **18**, 910 (1989).
31. P. M. LeClerq and D. M. Desiderio, *Org. Mass Spectrom.* **7**, 515 (1973).
32. C. W. Tsang and A. G. Harrison, *J. Am. Chem. Soc.* **98**, 1301 (1976).
33. W. Kulik and W. Heerma, *Biomed. Environ. Mass Spectrom.* **15**, 419 (1988).
34. S. Bouchonnet, J. P. Denhez, Y. Hoppilliard and C. Mauriac, *Anal. Chem.* **64**, 743 (1992).
35. G. Bouchoux, S. Bourcier, Y. Hoppilliard and C. Mauriac, *Org. Mass Spectrom.* **28**, 1064 (1993).
36. N. N. Dookeran, T. Yalcin and A. G. Harrison, *J. Mass Spectrom.* **31**, 500 (1996).
37. C. J. Proctor, B. Kralj, A. G. Brenton and J. H. Beynon, *Org. Mass Spectrom.* **15**, 619 (1980).